Nanoscale physico-chemical reactions at bioceramics-bone tissues interfaces

Edouard Jallot

Nanoscale physico-chemical reactions at bioceramics-bone tissues interfaces

JALLOT E.

Laboratoire de Physique Corpusculaire de Clermont-Ferrand CNRS/IN2P3 UMR 6533

Université Blaise Pascal, 24 avenue des Landais 63177 Aubière Cedex France

Tel : 33 (0)4 73 40 72 65

Fax : 33 (0)4 73 26 45 98

E-mail : jallot@clermont.in2p3.fr

Keywords : Biomaterials – Bioceramics – Calcium phosphates – Bioactive glasses – Biovitroceramics – Apatite – Precipitation – Dissolution – Physicochemical reactions

Contents

1. Introduction

The treatment of various pathologies in orthopaedic and dental surgery requires the implantation of a biomaterial to compensate for bone loss due to trauma and fracture and promote healing [1, 2]. Many materials have been developed for bone tissues replacement. They need to be stable for a long period of time and firmly fixed to bone [3, 4].

Actually, a lot of synthetic bone substitutes and prosthesis are available to repair bony tissues that are lost or damaged. The most widely used are polymers, metallic alloys (Ti6Al4V, Co-Cr, inox, …) and bioceramics (alumina (Al_2O_3), zirconia (ZrO_2), calcium phosphates, bioactive glasses, biovitroceramics) [5, 6]. The ultimate goal of these materials is to reach full integration of the non-living implant with living bone. With advances in ceramic technology, the application of calcium phosphate materials, bioactive glasses and biovitroceramics as bone substitutes or as coatings on prosthesis has received considerable attention, because they are highly biocompatible (well accepted in biological environment) and they have bioactive properties [7-9].

In orthopaedic and dental applications, calcium phosphate based ceramics, bioactive glasses, biovitroceramics and composites have been used by virtue of their ability to bond with bone tissues and to promote bone formation [10, 11]. These materials have become known as ‘bioactive ceramics’. They are capable, through physico-chemical reactions, to establish a direct contact with bone [12]. This concept of bonding through a thin or nonexistent interfacial layer permits to distinguish different types of bioactive materials (figure 1). As the chemical composition of calcium phosphate biomaterials is similar to that of vertebrate mineral phases (bone, dentin, etc.) [13, 14], they have proved to be efficient bone substitutes. Calcium-deficient apatite (CDA), hydroxyapatite (HA) and β-tricalcium phosphate are frequently used [15, 16] either alone or in association, e.g. biphasic calcium phosphate (BCP) [11, 17]. Bioactive glasses and biovitroceramics developed during the past

few decades have provided promising alternatives as materials to repair or replace parts of the skeletal system and as prosthetic coatings [18, 19]. Hench proved that bioactive glass (45 % SiO_2, 24.5 % CaO, 24.5 % Na_2O and 6 % P_2O_5) was able to bond to living bone due to the formation of an apatite layer on its surface [20]. Kokubo demonstrated similar reactions for bioactive ceramics which bonded to bone through an intervening apatite layer, suggesting chemical bonding [21, 22]. On the other, chemical treatment of Ti with NaOH aqueous solutions also creates surfaces that grow apatite layers and form a strong bond to bone [23, 24].

Together with the development of bioceramics, several efforts have been pursued in order to explain the mechanisms responsible for their *in vitro* and *in vivo* behaviours [25]. Many critical and complex reactions take place at the implant/bone tissues interface [26]. Structural and chemical evaluation at the nanometer scale of this interface is primordial to determine the success of an implant. Elemental composition and surface properties play a very important role in these reactions [27, 28]. Knowledge of the elemental distribution at the biomaterials/bone tissues interface is important to understand the physico-chemical mechanisms involved during the material integration and bone bonding [29, 30].

Scanning electron microscopy (SEM) and transmission electron microscopy (TEM) associated to energy dispersive X-ray spectroscopy (EDXS), X-ray photo-electron spectroscopy (XPS), electron energy loss spectroscopy (EELS) are methods which permits the analysis of bioceramics/bone tissues interface at the required resolution [31-35]. SEM, TEM and associated techniques are powerful tools which can provide chemical and physical information : morphology, interlayer thickness, chemical species, local bonding, and the nature of crystalline or amorphous products [36-39]. On the other hand, complementary techniques like PIXE (Particles induced X-ray emission), SIMS (Secondary ion mass spectrometry) and AFM (atomic force microscopy) are useful to better evaluate biomaterials/

bone tissues interface. PIXE and SIMS allow elemental mapping at the surface or at interfaces with a good spatial resolution. These methods are interesting to study trace elements locally at biomaterials interface [40]. AFM is used to study changes of surface morphology and roughness and even to determine adsorption of proteins on materials, surface rugosities induced by protein adsorption [41-44].

2. Physico-chemical reactions at calcium phosphate ceramics-bone tissues interface

Calcium phosphate ceramics are very used to repair bone defects or as prosthetic coatings [45, 46]. Coatings of metal implants with calcium phosphate materials combine the bioactive properties of the calcium phosphate material and the strength of the metal. Various types of calcium phosphate materials can be elaborated : dicalcium phosphate dihydrate (Brushite, $CaHPO_4.H_2O$), dicalcium phosphate anhydrous (Monetite, $CaHPO_4$), β-Tricalcium phosphate (β-TCP, $Ca_3(PO_4)_2$), Tetracalcium phosphate (TTCP, $Ca_4P_2O_9$), Octacalcium phosphate (OCP, $Ca_8H_2(PO_4)_6.5H_2O$), Calcium hydroxyapatite (HA, $Ca_{10}(PO_4)_6(OH)_2$), Calcium fluorapatite (FA, $Ca_{10}(PO_4)_6F_2$), … They are available in various physical forms: particles or blocks ; dense or porous. Coatings can be obtained by plasma spray, electrodeposition or dip coating of sol-gel preparations [47-52]. Macroporosities (pores > 100 μm) are created by the addition of volatile substances before sintering at high temperatures. Microporosities (pores < 10 μm) are induced by the sintering process, the time and the temperature. These materials differ in their solubility and physico-chemical reactions during their interactions with bone tissues. The most used in surgery and the most studied are hydroxyaptite, β Tricalcium phosphate.

2.1 Hydroxyapatite (HA) - β Tricalcium phosphate (β-TCP)

Synthetic hydroxyapatites are calcium phosphate ceramics elaborated by co-precipitation, by hydrolysis of acidic Ca-P compounds or by sol-gel process. Co-precipitation method consists of an aqueous hydrolysis under pressure and under temperature treatment of $Ca(NO_3)_2$, H_3PO_4, NH_4OH and H_2O [53]. The acidic Ca-P compounds include dicalcium phosphate dihydrate, dicalcium phosphate anhydrous and octacalcium phosphate [54, 55]. Sol-gel process used ethanol solutions with $Ca(NO_3)_2.4H_2O$ and P_2O_5 as Ca and P precursors respectively [56, 57].

This ceramic is used under different forms : powders, bulk or as coatings. For example, figure 2 shows a STEM micrograph of nanostructures of hydroxyapatite powders. For bulk materials, various porosities are available [58]. We can distinguish microporosities (<10 μm) which permit diffusion of ions and fluids from macroporosities (100-600 μm) which permit cellular colonisation. Macroporosities give osteoconductive properties to the ceramic.

When HA or β-TCP materials are in contact with living system (cells, fluids, …) they undergo biodegradation/biodissolution. This process results in physico-chemical changes like breaking into smaller particles, loss of mechanical strength, modification of micro- and macroporosities, modification of the implant size [59, 60]. The dissolution is principally caused by reduction in pH in the implant environment and can lead to changes in the materials at the micrometer and nanometer level. This phenomenon can be described as the bioactivity process [61, 62].

The bioactivity process was studied *in vitro* and *in vivo* [33, 63-66]. It occurs under an acidic attack with H^+ at the material surface [67]. The correlation between dissolution in acellular conditions *in vitro* and in cell-mediated dissolution (biodegradation/bioresorption) in

cell culture and *in vivo* comes from the fact that both processes (cellular or acellular) are caused by acidic conditions [68, 69]. The acidic attack leads to the dissolution of hydroxyapatite : changes in porosity, density, loss of material, changes in particles diameter and average crystals size [63]. This dissolution results in a high release of Ca^{2+}, PO_4^{3-} ions into the surrounding fluids and tissues [15, 70]. These ions are free to combine with other ions from biological fluids to form other calcium phosphate phases. Concentrations of calcium and phosphorus increase in the surrounding fluids and this supersaturation induces reprecipitation of other apatite crystals (brushite, octacalcium phosphate, carbonated-hydroxyapatite …) at the ceramic surface [71]. These apatite crystals may incorporate Ca^{2+}, Mg^{2+}, CO_3^{2-}, PO_4^{3-}, F^- and organic molecules present in the surrounding fluids [72, 73]. The presence of Mg^{2+} stabilizes brushite, octacalcium phosphate and reduces their transformation into apatite [74]. On the other hand, CO_3^{2-}, F^- and some protein molecules can promote the formation of apatite [75]. This dissolution-reprecipitation process leads to the formation of a carbonated apatite layer at the material surface. This layer is in the order of 200-800 nm [76-77]. Then, an extra-cellular matrix (collagenous and non-collagenous proteins) is produced. This is followed by the mineralization of collagen fibrils together with the incorporation of the newly formed apatite crystals in the newly formed bone [78, 79]. These reactions permit a strong chemical bond with newly formed bone at the implant/bone interface [33].

Solubility of hydroxyapatites varies with different factors : porosity, grain size, crystallinity, sintering temperature … [80-84]. The solubility increases with the porosity and pores size [85]. Porous hydroxyapatite dissolves more rapidly than dense hydroxyapatite [86]. An increase of the sintering temperature leads to an increase of the hydroxyapatite crystals size and reduces the number of lattice defects. For example, hydroxyapatite treated at 600°C has crystals of 180 nm in size and crystals of 350 nm in size with a treatment at 1180°C [82]. Smaller crystals will dissolve more rapidly than larger crystals of the same composition, due

to the surface area exposed to the biological environment and to the greater number of lattice defects [15, 83, 87-89]. Moreover, the grain boundaries without lattice continuity could be more soluble than grain boundaries with a lattice continuity [15, 84]. The presence and characteristics of the grain boundaries are also influence by sintering temperature and duration. In addition, the crystalline phase and ionic substitution can influence the dissolution process [90, 91]. It has been demonstrated that β-TCP is more soluble and biodegrades to a greater extend than HA [92].

2.2 Biphasic calcium phosphate ceramics (BCP)

With biphasic calcium phosphate ceramics, Daculsi developed a bioactive concept. This concept is base on an optimum balance of the more stable phase of HA and more soluble β-TCP [17]. To prepare BCP a mixture of HA and β-TCP is prepared by precipitation or co-precipitation and sintered at 1100°C. BCP with varying β-TCP/HA ratios can be prepared by sintering precipitated calcium deficient apatites of varying Ca/P ratios [33, 93, 94]. These calcium deficient apatites can be elaborated by precipitation of dicalcium phosphate dihydrate ($CaHPO_4.2H_2O$) or dicalcium phosphate anhydrous ($CaHPO_4$) or octacalcium phosphate ($Ca_8H_2(PO_4).5H_2O$) [95]

This material is soluble and gradually dissolves when it is in contact with bone tissues. Its dissolution depends on the β-TCP/HA and concerns the individual HA or β-TCP crystals [15, 33]. During dissolution, the proportion of HA to β-TCP crystals in BCP appeared greater and the decrease in average size of crystals is associated with an increase in the size of macroporosity [96]. Daculsi demonstrated for the first time that the new microcrystals were not necessarily deposited on collagenous fibers and a process of calcification occurs through the formation of carbonate apatites in association with the CaP ceramics without cell differenciation [97]. The formation of these carbonated apatites occurs through the HA or β-

TCP crystals dissolution and precipitation under certain supersaturation conditions. The precipitation occurs at the periphery of the HA or β-TCP crystals and forms a layer. These reactions lead to new bone formation together with the release of calcium and phosphate ions into the surrounding biological fluids [94-99]. The new bone is firmly bonded to the biomaterials through the carbonate apatite layer and progressively replaces the materials. This bond becomes reinforced by the crystal-protein affinity.

3. Physico-chemical reactions at bioactive glasses-bone tissues interface

3.1 Definition of bioactive glasses

In 1970, Hench [20] [100] discovers the bioactive glasses. They are amorphous materials with low mechanical properties which reduces their applications to prosthetic coatings [101, 102] and to fill bony defects [103-105]. Bone bonding was first demonstrated for a certain compositional range of bioactive glasses that contained SiO_2, CaO, Na_2O and P_2O_5 [20]. The bioactivity properties of these materials depend on the percentage of these three oxides : SiO_2, CaO, Na_2O. Figure 3 shows the compositional dependence of bone bonding for the SiO_2-CaO-Na_2O-P_2O_5 system [106]. Compositions in region A, are bioactive and bond to bone. The concentration of SiO_2 must be less than 60 mol% together with a high CaO and Na_2O content and a high CaO/P_2O_5 ratio. Glasses with high amount of P_2O_5 do not bond to bone tissues. These compositional definitions lead to a highly reactive material when exposed to a biological environment. The most known composition is based upon the formula called '45S5' : (45%) SiO_2, (24.5%) CaO, (24.5%) Na_2O and (6%) P_2O_5. In region E, bioactive glasses are able to bond strongly to collagenous constituent of soft tissues. In region B, a high increase of SiO_2 leads to the formation of classical glasses which are bio-inert material [107] (figure 3). The interfacial reactions result in the formation of a fibrous capsule at the material-bone tissues interface. Region C defines glasses which are resorbable and

disappear within 10-30 days of implantation [106]. An increase of CaO or Na_2O leads to a non-glass material (region D). In fact, a very limited range of bioactive glass compositions, containing SiO_2-CaO-Na_2O-P_2O_5, that have less than 60% SiO_2 exhibit a high bioactivity and bond to both bone and soft connective tissues [108].

Bioactive glasses can be obtained by melting the components at 1350°C or by sol-gel method at a lower temperature [109]. The synthesis of bioactive glasses by sol-gel process was proposed in the last decade [110, 111]. The solutions to obtain bioactive gel-glasses were prepared from stoichiometric amounts of tetraethoxysilane, triethyl phosphate and $Ca(NO_3)_2.4H_2O$. Hydrolysis and condensation at low temperature create a highly interconnected 3-D gel network composed of $(SiO_4)^{4-}$ tetrahedral via bridging oxygen bonds or by Si-O-Ca or Si-O-P non-bridging bonds [112-115].

3.2 Kinetics of interfacial reactions

Interfacial reactions during bonding to bone tissues have been studied *in vitro* during interactions between bioactive glasses and biological fluids (table 1) or *in vivo* during interactions with bony tissues [116-121]. The bone bonding process can be decomposed in 11 stages. At the bioactive glass-bone interface a complex series of physico-chemical reactions including dissolution, diffusion, ionic exchange, precipitation occurs according to time of interaction together with cellular events which lead to the rapid formation of new bone (figures 4 and 5) [122-126]:

- Stage 1: Rapid exchange of alkali ions (Na^+ or K^+) with H^+ or H_3O^+ from surrounding fluids through an exchange layer of the order of 200 nm [30, 37]. The exchange process consist of a flow of H_3O^+ ions and an equivalent flow of sodium ions into the solution from the glass represented as follow :

$$\text{Si-O-Na}^+ + \text{H}_3\text{O}^+ \rightarrow \text{Si-OH} + \text{H}_2\text{O} + \text{Na}^+_{(\text{solution})}$$

This stage is usually controlled by diffusion and exhibits a $t^{-1/2}$ dependence.

- Stage 2 : Loss of soluble Si to the solution resulting from breaking of Si-O-Si bonds. Soluble silicon migrates toward the surface and there is formation of Si-OH (silanols) and Si-$(OH)_4$ groups at the surface :

$$\text{Si-O-Si} + H_2O \rightarrow \text{Si-OH} + \text{OH-Si}$$

- Stage 3 : Condensation and repolymerisation of a hydrated Si rich layer on the surface depleted in alkali and Ca,P elements. This layer is a vitreous gel and growth by alkali ions exchange [43].

- Stage 4 : Migration of Ca and P from the glass to the surface trough the Si layer. Several authors described this phenomenon as a diffusion process through the Si rich layer. Formation of a Ca-P film on top of the Si layer, followed by growth of an amorphous Ca-P rich film by incorporation of soluble calcium and phosphate from the bulk material and from the surrounding biological fluids.

- Stage 5 : Crystallization of an hydroxyl carbonate apatite (HCA) layer on top of the Si layer. Growth of the HCA layer [127]. At the beginning the apatite crystals size is of the order of 200 nm. The size of the HCA layer increases to some micrometers by consuming Ca^{2+}, PO_4^{3-}, CO_3^{2-}, HPO_4^{2-}, OH^- from surrounding fluids. The characteristic double layer formation (stage I-V) on the surface of a bioactive glass is schematically shown in figure 5.

- Stage 6 : Adsorption and desorption of biological growth factors in the HCA layer from surrounding tissues. This incorporation of biochemical growth factors activate differentiation of stem cells.

- Stage 7 : Action of macrophages to remove debris from the site allowing cells to occupy the space.

- Stage 8 : Attachment of stem cells on the bioactive glass surface.

- Stage 9 : Differentiation of stem cells to form bone growing cells, such as osteoblasts.
- Stage 10 : Generation of extra cellular matrix by the osteoblasts to form bone.
- Stage 11 : Crystallisation of inorganic calcium phosphate matrix to enclose bone cells in a living composite structure.

Formation and growth of this biological apatite layer *in situ* represents the bioactivity properties and permits a chemical link between the materials and the newly formed bone. The formation of this layer occurs very rapidly and the delay depends on the bioactive glasses composition which influences greatly its dissolution. Reaction stages 1 and 2 are responsible for the dissolution of a bioactive glass and therefore influence the rate of HCA layer formation. At the periphery of the 45S5 glass, it has been demonstrated that, after only 1 h a Ca-P rich layer begins to develop [128]. The apatite crystals of the HCA layer and the apatite crystals of the newly formed bone are intermingled each others which leads to the high bonding strength of the interface [129]. For example, figure 6 shows bioactive glass particles immersed four days in biological fluids. Interactions between bioactive glass particles and the fluids lead to the materials dissolution, to the formation of a Si layer and finally to the precipitation of an apatite layer. On the STEM micrograph, this layer appears as an electron dense layer. At this short time period, the apatite layer is of the order of 500 nm in thickness and its size will increases with time. In case of a crystallised apatite layer, a needle shape like structure will appear. EDXS spectrum on this layer demonstrates the presence of Ca and P elements. The apatite layer acts as a template for bone cells adhesion and differentiation [119].

For bioactive implants, it is necessary to be able to control the solubility of the material. A low solubility material is necessary if the implant is designed to have a long life

and is used as coating on metals alloys like titanium. In order to improve the long-term stability of the glass and to reduce the glass networks dissolution which occurs within days, addition of other elements can be done. Optimisation of bioactive glasses properties concerns the compromise between bioactivity and solubility which is related to individual components [130-132]. For example, addition of Al_2O_3 can be used to control the solubility of the glass without altering the surface reaction kinetics of the material. However, this addition may inhibit the bone bonding [133]. Greenspan and Hench demonstrate that a concentration of Al_2O_3 higher than 2% inhibits bioactivity [134].

3.3 Sol-gel derived bioactive glasses

No melt derived glasses with more than 60 mol% SiO_2 are bioactive. In order to obtain bioactivity for silica levels higher than 60 mol% the sol-gel process must be employed.

In case of bioactive gel-glasses derived materials, the 1-10 nm scale solid network of the gel is completely interpenetrated by pore liquid. The pore liquid consists of a highly structured hydrated layer with hydrated connective tissues. Biological molecules can exchange with these hydrated layers inside the pores and maintain their structure together with their biological properties [135, 136]. The nanometer sized pores of the gel glass are proposed to act as initiation sites for apatite nucleation [137]. Bioactive glasses elaborated by sol-gel process permit an increase of HCA formation and higher bioactivity [138-140]. This is attributed to a higher release of soluble silica that nucleates HCA crystals in the nanometer sized pores of the gel [141]. Pore sizes greater than 2 nm were required to achieve rapid kinetics for HCA layer formation. Moreover, an increase of the surface area lead to an increase of the surface exposed to biological fluids, improving ion exchange (stage 1) and a greater release of soluble silica (stage 2) that is required to form a porous silica rich layer. The

extended of SiO_2 composition range from 60% to 90% of bioactive glasses is supposed to come from the specific porous structure of sol-gel derived glasses.

Hench demonstrates that chemical composition, amount of glass phase and solubility can be used to classify bioactive materials [142]. He classified bioactive materials into two classes : class A is osteoproductive and class B is osteoconductive [12]. Class A releases Si under silicic acid form due to ion exchange and network dissolution, and rapidly provides a Si layer which permits the precipitation of an amorphous Ca-P layer and finally cristallisation of a HCA layer. This class of glasses elicits bone and soft tissues bonding with proliferation and differentiation of osteoprogenitor cells. Class B has low or zero rate of Si release and forms a HCA layer more slowly than class A. This class only shows bone bonding.

4. Physico-chemical reactions at biovitroceramics-bone tissues interface

4.1 Definition of biovitroceramics

In 1982, Yamamuro and Kokubo develop bioactive glass-ceramics or called 'biovitroceramics' [143-146]. A vitro ceramic is obtained by a temperature treatment of a glass in which nucleation factors are added in order to induce a partial or total crystallisation of this glass. This glass-ceramic has excellent mechanical properties. A biovitroceramic has a structure and a particular chemical composition which are crucial for the bioactivity properties. Three types of biovitroceramics can be elaborated [147, 148] :

- Biovitroceramics composed with a vitreous matrix ((16.6%) MgO, (24.2%) CaO, (59.2%) SiO_2) in which apatite crystals (oxyfluoroapatite : $Ca_{10}(PO_4)_6(O,F_2)$ are incorporated.

- Biovitroceramics (A-W) composed with a vitreous matrix in which apatite crystals and β-wollastonite crystals ($CaSiO_3$) are incorporated.

- Biovitroceramics composed with a vitreous matrix in which apatite crystals, β-wollastonite crystals and whitelockite crystals ($3CaOP_2O_5$) are incorporated.

4.2 Kinetics of interfacial reactions

Studies of the bioactivity was made *in vitro* during interactions between biovitroceramics and biological fluids, and *in vivo* during interactions between biovitroceramics and bone [29, 149-153]. The bioactivity process is based on (figure 7) :

- Dissolution of the vitreous matrix, wollastonite crystals and whitelockite crystals (if they are incorporated).

- Ionic release of $HSiO_3^-$, Ca^{2+}, Mg^{2+} at the surface.

- Precipitation of an apatite (Ca-P) layer by consuming Ca^{2+}, PO_4^{3-}, CO_3^{2-}, and HPO_4^{2-} from biological fluids. After 7 days, the A-W ceramics is completely covered by a layer of apatite. The Ca-P rich layer consists of a carbonate containing hydroxyapatite of small crystallites.

The apatite phase present in the glass-ceramic does not play an important role during physico-chemical reactions at the bioceramic periphery and the formation of an apatite layer on its surface [29]. In fact, ions released from the vitreous matrix and from wollastonite play an important role in forming the apatite layer on their surface. The Ca-P layer is formed by a chemical reaction of the glass-ceramic with surrounding fluids, in which organic substances such as cells and proteins take little part [29]. The formation of this apatite layer at the surface of biovitroceramics occurs without the formation of a Si-rich layer even though a substantial concentration of soluble silicon was lost to solution [149]. However, calcium and silicate ions dissolved from the glass–ceramic cooperatively play an important role in forming the apatite

layer on its surface in the body environment. The calcium ions might increase the degree of supersaturation of surrounding body fluids with respect to the apatite precipitation [29]. Silicate ions might provide favourable sites for nucleation of the apatite on the biovitroceramics surface because the apatite is only formed on the surface [154]. Phosphate ions required for the formation of the apatite layer are supplied only from the surrounding fluids (figure 7). The Ca-P layer of some micrometers in thickness permits a chemical bond between the materials and the newly formed bone (figure 8). Kokubo demonstrates that the Ca-P layer at the interface plays the essential role in forming the chemical and strong bond of the glass-ceramics to the bone [155].

5. Physico-chemical reactions at bioactive titanium surface

Metals like titanium and its alloys are biocompatible materials which are clinically used as bone substitutes under high loading conditions. However, no direct chemical bond is formed at the interface between these materials and bone. In order to give bioactive surface properties to these biomaterials various methods are used [156, 157]. The most known are elaboration with physical methods of coatings with bioactive materials like hydroxyapatite or bioactive glasses [158, 159]. Unfortunately it is difficult to control quality of the coatings [160, 161]. Recently, it has been found that even pure titania hydrogel prepared by sol-gel method induces apatite formation [162-164].

When titanium is treated by immersion in alkaline solution (NaOH), a hydrated titanium oxide gel layer containing alkali ions is formed on its surface. This gel layer is dehydrated and densified to form an amorphous alkali titanate ($TiO_2 + Na^+$) layer by heat treatment below 600°C. When the pre-treated titanium is exposed to biological fluids, the alkali ions are released from the amorphous alkali titanate layer and hydronium ions enter into the surface layer, resulting in the formation of a titanium oxide hydrogel layer. The released

Na^+ ions increase the degree of supersaturation of the soaking solution with respect to apatite by increasing pH, and titanium oxide hydrogel induces apatite nucleation on the titanium surface [165]. Figure 9 schematised possible structural changes of the titanium surface during chemical treatment and subsequent apatite formation in simulated body fluids (SBF) [162] :

a – Generally, the surface of titanium is covered with a thin passive titanium oxide layer.

b – During acidic etching, this TiO_2 passive layer dissolves to form TiH_2. In contact with air moisture a new titanium oxide layer is formed. This layer is thinner than the original one.

c – In alkali solution, however, even this thin passive layer dissolves to form an amorphous layer containing Na^+ ions.

d to f – Upon exposure to SBF, the thus treated titanium releases Na^+ ions from the surface via ion exchange with Ca^{2+} from the surrounding fluids. Subsequently, the incorporation of PO_4^{3-}, CO_3^{2-} occurs which leads to an HCA layer. The amorphous TiO_2-layer formed on the surface induces the apatite nucleation. The released Na^+ ions accelerate the apatite nucleation by increasing the ionic activity of apatite due to increasing pH [166]

Conclusion

Bioactive ceramics differ in composition and physico-chemical properties from each other and from bone. These differences must be taken into consideration for a better bone growth at the expense of biomaterials and to adapt to new development of specific biomaterials. Characterisation of bioceramics/bone tissues interface in terms of physico-chemical properties and cellular response is important to better understand events occurring at bone/bioceramic interface [167]. A sequence of events at the surface of the bioactive materials promotes bone bonding resulting in a uniquely strong and intimate bone/materials

interface. The sequence of events differs with the materials and includes : (1) biodissolution / biodegradation / bioresorption of bioactive material by extracellular and intracellular interactions; (2) formation through physico-chemical reactions / reprecipitation of apatite microcrytals (intimately associated with the organic matrix) at the surface of bioactive materials ; (3) mineralization of the collagen fibrils and incorporation of the new apatite crystals in the newly formed bone. However, a common characteristic of bioactive materials is a time-dependent, kinetic modification of the surface that occurs during interactions with bone tissues. The surface forms a biologically active (hydroxycarbonate) apatite layer of nanometer scale that permits a firm bone bonding. This apatite layer is chemically and structurally equivalent to the mineral phase of bone which allows an interfacial bonding [168-170]. This bioactive fixation has strength equal to or greater than bone after 3-6 months. The rate of apatite layer formation and the time for onset of crystallisation varies greatly with the bioactive materials composition [171]. When the rate becomes excessively slow, no bond forms, and the material is no longer bioactive. This bonding rate and thickness of interfacial bonding layers permits to define and to develop many bioactive materials with specific properties (figure 1). This new generation of bioactive materials should increase the quality of life of millions of people as the life expectancy increase.

References

1. C. Nicolazo, H. Gautier, M.J. Brandao, G. Daculsi and C. Merle, *Biomaterials* 24, 255 (2003).

2. M.B. Habal and A.H. Reddi, Bone grafts and bone substitutes, W.B. Saunders Company, Philadelphia, 1992.

3. Y. Fujishiro, L.L. Hench and H. Oonishi, *J. Mater. Sci-Mater. Med*. 8, 649 (1997).

4. A.M. Gatti, G. Valdre and A. Tombesi, *J. Biomed. Mater. Res.* 31, 475 (1996).

5. L.L. Hench, *J. Am. Ceram. Soc.* 74, 1487 (1991).

6. E. Jallot, H. Benhayoune, G. Weber, G. Balossier and P. Bonhomme, *J. Phys. D : Appl. Phys.* 33, 321 (2000).

7. M. Jarcho, *Clin. Orthop. Relat. Res.* 157, 259 (1981).

8. R.Z. Legeros, *Adv. Dent. Res.* 2, 164 (1988).

9. C. Ohtsuki, T. Kokubo and T. Yamamuro, *J. Am. Ceram. Soc.* 75, 2094 (1992).

10. E. Jallot, *J. Advanced Materials* 35, 9 (2003).

11. G. Daculsi, N. Passuti, S. Martin, C. Deudon, R.Z. Legeros and S. Raher, *J. Biomed. Mater. Res.* 24, 379 (1990).

12. L.L. Hench, *Biomaterials* 19, 1419 (1998).

13. K.L. Lawson, K.E. Marks and J. Brems, *Orthopedics* 13, 521 (1990).

14. R.Z. Legeros, 'Hydroxyapatite and related materials' (P.W. Brown and B. Constantz, Eds), CRC Press, Boca Raton: FL, 1994.

15. G. Daculsi, R.Z. Legeros and D. Mitre, *Calcified Tissue Int.* 45, 95 (1989).

16. G. Daculsi and N. Passuti, *Biomaterials* 11, 86 (1990).

17. G. Daculsi, *Biomaterials* 19, 1473 (1998).

18. L.L. Hench and J.K. West, *Life Chemistry Reports* 13, 187 (1996).

19. T. Kokubo, ‘In introduction to bioceramics’ (L.L. Hench and J. Wilson, Eds), London and Singapore : World Scientific 75 (1993).

20. L.L. Hench, R.J. Splinter, T.K. Greenlee and W.C. Allen, *J. Biomed. Mater. Res.* 5, 117 (1971).

21. T. Kokubo, *Biomaterials* 12, 155 (1991).

22. M. Neo, S. Kotani, T. Nakamura, T. Yamamuro, C. Ohtsuki, T. Kokubo and Y. Bando, *J. Biomed. Mater. Res.* 26, 1419 (1992).

23. H.M. Kim, F. Miyaji, T. Kokubo and T. Nakamura, *J. Biomed. Mater. Res.* 32, 409 (1996).

24 F. Liang, L. Zhou and K. Wang, *Surface and Coatings Technology* 165, 133 (2003).

25. O.H. Andersson and K.H. Karlsson, *J Non-Cryst. Solids* 129, 145 (1991).

26. T. Kitsugi, T. Nakamura, M. Oka, Y. Senaha, T. Goto and T. Shibuya, *J. Biomed. Mater. Res.* 30, 261 (1996).

27. F.L.S. Carvalho, C.S. Borges, J.R.T. Branco and M.M. Pereira, *J. Non-Cryst. Solids* 247, 64 (1999).

28. V.K. Marghussian and A. Sheikh-Mehdi Mesgar, *Ceramics International* 26, 415 (2000).

29. T. Kokubo, *J. Non-Cryst. Solids* 120, 138 (1990).

30. E. Jallot, H. Benhayoune, L. Kilian and Y. Josset, *Langmuir* 19, 3840 (2003)

31. J.I. Goldstein, J.L. Costley, G.W. Lorimer and S.J.B. Reed in Scanning Electron Microscopy edited O. Johari, IITRI, Chicago (1977), Vol. 1, p. 135.

32. C. Otsuki, Y. Aoki, T. Kokubo, Y. Bando, M. Neo and T. Nakamura, *J. Am. Ceram. Soc.* 103, 449 (1995).

33. R.Z. Legeros and G. Daculsi, in ‘Handbook of bioactive ceramics’ (T. Yamamuro, L.L. Hench and J. Wilson, eds) Vol. 2, CRC Press, Boca raton 1990.

34. C.C. Gray, J.N. Chapman, W.A.P. Nicholson, B.W. Robertson and R.P. Ferrier, *X-ray Spectrom.* 12, 163 (1983).

35. J.N. Chapman, C.C. Gray, B.W. Robertson and W.A.P. Nicholson, *X-ray Spectrom*. 12, 153 (1983).

36. M. Neo, T. Nakamura, T. Kikutani, K. Kawanabe and T. Kokubo, *J. Biomed. Mater. Res.* 27, 999 (1993).

37. E. Jallot, H. Benhayoune, L. Kilian, Y. Josset and G. Balossier, *Langmuir* 17, 4467 (2001).

38. R.D. Leapman and R.L Ornberg, *Ultramicroscopy* 24, 251 (1988).

39. E.I. Suvorova and P.A. Buffat, *J. Microsc* 196, 46 (1999).

40. E. Jallot, J.L. Irigaray, H. Oudadesse, V. Brun, G. Weber and P. Frayssinet, *Nucl. Instrum. Meth. B* 142,156 (1998).

41. M. Collaud Coen, R. Lehmann, P. Gröning, M. Bielmann, C. Galli and L. Schlapbach, *J. Colloid and Interf. Sci.* 233, 180 (2001).

42. A. Ikai, *Surf. Sci. Rep.* 26, 261 (1996).

43. E. Saiz, M. Goldman, J.M. Gomez-Vega, A.P. Tomsia, G.W. Marshall and S.J. Marshall, *Biomaterials* 23, 3749 (2002).

44. A. Itälä, E.C. Nordstöm, H. Ylänen, H.T. Aro and M. Hupa, *J. Biomed. Mater. Res.* 56, 282 (2001).

45. E. Jallot, J.L. Irigaray, H. Oudadesse, V. Brun, G. Weber and P. Frayssinet, *Eur. Phys. J. AP* 6, 205 (1999).

46. R.Z. Legeros, *Clinical Materials* 14, 65 (1993).

47. D.M. Liu, T. Troczynski and W. J. Tseng, *Biomaterials* 22, 1721 (2001).

48. S.W.K. Kweh, K.A. Khor and P. Cheang, *Biomaterials* 23, 775 (2002).

49. S. Kaciulis, G. Mattogno, L. Pandolfi, M. Cavalli, G. Gnappi and A. Montenero, *Applied Surface Science* 151, 1 (1999).

50. W. Wenjian and J. L. Baptista, *Biomaterials* 19, 125 (1998).

51. H. Benhayoune, P. Laquerriere, J.L. Bubendorff, E. Jallot, G.D. Sockalingum, A. Perchet, L. Kilian and G. Balossier, *J. Mater. Sci-Mater. Med.* 13, 1057 (2002).

52. E. Milella, F. Cosentino, A. Licciulli and C. Massaro, *Biomaterials* 22, 1425 (2001).

53. R. Aoba and E.C. Moreno, *J. Dent. Res.* 63, 874 (1984).

54. R.Z. LeGeros, J.P. LeGeros, O.R. Trautz and W.P. Shirra, *Adv. X-ray Anal.* 14, 57 (1971).

55. R.Z. LeGeros, G. Daculsi, I. Orly, T. Abergas and W. Torres, *Scan. Microsc.* 3, 129 (1989).

56. W. Weng, S. Zhang, K. Cheng, H. Qu, P. Du, G. Shen, J. Yuan and G. Han, *Surface and Coatings Technology* 167, 292 (2003).

57. K. Cheng, G. Shen, W. Weng, G. Han, J.M.F. Ferreira and J. Yang, *Materials Letters* 51, 37 (2001).

58. P.S. Eggli, W. Muller and R.K. Schenk, *Clin. Orthopd. Relat.* 232, 127 (1988).

59. H.W. Denissen, W. Kalk, H.M. De Nieuport, J.C. Maltha and H. Van de Hoof, *Int. J. Prosthodont.* 3, 53 (1990).

60. C.M. Muller-Mai and U. Gross, *Scan. Microsc.* 4, 613 (1990).

61. B.M. Tracy and R.H. Doremus, *J. Biomed. Mater. Res.* 18, 719 (1984).

62. P. Ducheyne and K. De Groot, *J. Biomed. Mater. Res.* 15, 441 (1981).

63. C.P.A.T. Klein, K. De Groot, A.A. Driessen and H.B.M. Lubbe, *Biomaterials* 6, 189 (1985).

64. C.P.A.T. Klein, K. De Groot, A.A. Driessen and H.B.M. Lubbe, *Biomaterials* 7, 144 (1986).

65. I. Orly, M. Gregoire, M. Menanteau and M. Dard, *Adv. Biomater.* 8, 211 (1988).

66. E. Jallot, *Med. Eng. Phys.* 20, 697 (1998).

67. G. Daculsi, G. Kerebel and L.M. Kerebel, *Caries Res.* 13, 277 (1979).

68. H.S. Cheung and D.J. McCarty, *Experiment. Cell. Res.* 157, 63 (1985).

69. R.W. Evans, H.S. Cheung and D.J. McCarty, *Calcified Tissue Int. 36, 645 (1984).*

70. R.Z. Legeros, I. Orly, M. Gregoire and J. Kaimiroff, *J. Dent. Res*. 67, 177 (1988).

71. I. Orly, M. Gregoire, M. Menanteau, M. Heughebaert and B. Kerebel, *Calcified Tissue Int.* 45, 20 (1989).

72. R.Z. Legeros, M.H. Taheri, G.M. Quirolgico and J.P. Legeros, *Scanning Electron Microsc.* 407 (1983).

73. R.Z. Legeros, R. Kijkowska, T. Abergas and J.P. Legeros, *J. Dent. Res.* 65, 293 (1986).

74. R.E. Wuthier, G.S. Rice, J.E.B. Wallace, R.L. Weaver, R.Z. Legeros and E.D. Eanes, *Calcified Tissue Int.* 37, 401 (1981).

75. H. Fleisch, *J. Crystal Growth* 53, 120 (1981).

76. H.N. Denissen, K. De Groot, P.C. Makkes, A. Van Den Hoof and P.J. Klopper, *J. Biomed. Mater. Res.* 14, 730 (1980).

77. J.M. Sautier, J.R. Nefussi and N. Forest, *Cells and Materials* 1, 209 (1991).

78. J.M. Sautier, J.R. Nefussi and N. Forest, *Biomaterials* 12, 400 (1992).

79. G.C.L. De Lange, C. De Putter and F.L.J.A. De Wijs, *J. Biomed. Mater. Res.* 24, 829 (1990).

80. K. De Groot, *Ann. New York Acad. Sci.* 523, 227 (1988).

81. R.Z. Legeros and X. F. Chang, *J. Dent. Res.* 68, 215 (1989).

82. P. Laquerrière, L. Kilian, A. Bouchot, E. Jallot, A. Grandjean, M. Guenounou, G. Balossier, P. Frayssinet and P. Bonhomme, *J. Biomed. Mater. Res.* 58, 238 (2001).

83. G. Daculsi, R.Z. Legeros, J.P. Legeros, D. Mitre, *J. Biomed. Mater. Res.* 2, 147 (1991).

84. F.C.M. Driessens, in ‘Formation and stability of calcium phosphates in relation to the phase composition of the mineral in calcified tissues’ (K. De Groot, ed) Bioceramics of calcium phosphate, CRC Press, Boca Raton 1983.

85. C.P.A.T. Klein, A.A. Driessen, K. De Groot and A. Van Den Hoof, *J. Biomed. Mater. Res.* 17, 769 (1983).

86. H. Benhayoune, E. Jallot, P. Laquerrière, G. Balossier, P. Bonhomme and P. Frayssinet, *Biomaterials* 21, 235 (2000).

87. H.E. Lundager Madsen, F. Christensson, L.E. Polyak, E.I. Suvorova, M.O. Kliya and A.A Chernov, *J. Cryst. Growth* 152, 191 (1995).

88. E.I. Suvorova, F. Christensson, H.E. Lundager Madsen, A.A. Chernov, *J. Cryst. Growth* 186, 262 (1998).

89. C.P.A.T. Klein, A.A. Driessen and K. De Groot, *Biomaterials* 5, 157 (1984).

90. R.Z. Legeros in Tooth enamel IV edited R.W. Fearnhead and S. Suga, Elsevier, Amsterdam (1984), p. 32.

91. R.Z. Legeros and R. Kijkowska, *J. Dent. Res.* 68, 1003 (1989).

92. A.A. Driessen, C.P.A.T. Klein and K. De Groot, *Biomaterials* 3, 113 (1982).

93. O. Malard, J.M. Bouler, J. Guicheux, D. Heymann, P. Pilet, C. Coquard, G. Daculsi, *J. Biomed. Mater. Res.* 46, 103 (1999).

94. G. Daculsi, R.Z. Legeros, E. Nery, K. Lynch and B. Kerebel, *J. Biomed. Mat. Res.* 23, 883 (1989).

95. R.Z. Legeros, in ‘Monographs in Oral Sciences’ (H. Myers, S. Karger, eds) Vol. 15 Basel 1991.

96. G. Daculsi, R.Z. Legeros and D. Mitre, *Calcified Tissue Int.* 45, 95 (1989).

97. M. Heughebaert, R.Z. Legeros, M. Gineste, A. Guilhem and G. Bonel, *J. Biomed. Mat. Res.* 22, 257 (1988).

98. G. Daculsi, R.Z. Legeros, M. Heughebaert and I. Barbieux, *Calcified Tissue Int.* 46, 20 (1990).

99. E. Jallot, J.L. Irigaray, G. Weber and P. Frayssinet, *Surf. Interf. Anal.* 27, 648 (1999).

100. L.L. Hench, *Med. Inst.* 57, 136 (1973).

101. R.J. Furlong and J.F. Osborn, *J. Bone Joint Surg.* 77, 534 (1995).

102. A. Merolli, A. Cacchioli, L. Giannotta and P. Tranquilli Leali, *J. Mater. Sci-Mater. Med.* 12, 727 (2001).

103. E. Shepers, M. De Clerq, P. Ducheyne and R. Kempeneers, *J. Oral Rehabil.* 18, 439 (1991).

104. Ö.H. Andersson, K.H. Karlsonn and K. Kangasniemi, *J. Non-Cryst. Solids* 119, 290 (1990).

105. Ö.H. Andersson, G. Liu, K. Kangasniemi, J. Juhanoja, *J. Mater. Sci-Mater. Med.* 3, 145 (1992).

106. L.L. Hench, *J. Am. Ceram. Soc.* 81, 1705, (1998)

107. L.L. Hench in Handbook of bioactive ceramics edited T. Yamamuro, L.L. Hench and J. Wilson, CRC Press, Boca raton (1990), Vol. 1, p. 7.

108. W. Cao and L.L. Hench, *Ceramics Int.* 22, 493 (1996).

109. W. Gong, A. Abdelouas and W. Lutze, *J. Biomed. Mater. Res.* 54, 320 (2001).

110. R. Viitala, M. Jokinen, T. Peltola, K. Gunnelius and J.B. Rosenholm, *Biomaterials* 23, 3073 (2002).

111. C. Kinowski, M. Bouazaoui, R. Bechara, L.L. Hench, J.M. Nedelec and S. Turell, *J. Non-cryst. Solids* 291, 143 (2002).

112. L.L. Hench and R. Orefice in Kirk-Othmer encyclopedia of chemical technology, Wiley, New York, (1997) 4th ed., Vol. 22, p. 497.

113. R. Li, A.E. Clark and L.L. Hench in Chemical processing of advanced materials edited L.L. Hench and J.K. West, Wiley, New York, (1992), p. 627.

114. M.M. Pereira, A.E. Clark and L.L. Hench, *J. Mater. Synth. Proc.* 2, 189 (1994).

115. M.M. Pereira, A.E. Clark and L.L. Hench, *J. Biomed. Mater. Res.* 18, 693 (1994).

116. E. Jallot, H. Benhayoune, L. Kilian, J.L. Irigaray, H. Oudadesse, G. Balossier, P. Bonhomme, *Surf. Interf. Anal.* 29, 314 (2000).

117. L.L. Hench and J. Wilson, *Science* 226, 630 (1984).

118. C.Y. Kim, A.E. Clark and L.L. Hench, *J. Non-Cryst. Solids* 113, 195 (1988).

119. C. Loty, J.M. Sautier, M.T. Tan, M. Oboeuf, E. Jallot, H. Boulekbache, D. Greenspan and N. Forest, *J. Bone Miner. Res.* 16, 231 (2001).

120. A. El Ghannam, P. Ducheyne and I.M. Shapiro, *J. Biomed. Mater. Res.* 29, 359 (1995).

121. T. Kokubo, H. Kushitani, S. Sakka, T. Kitsugi and T. Yamamuro, *J. Biomed. Mater. Res.* 24, 721 (1990).

122. I.D. Xynos, A.J. Edgar, L.D.K. Buttery, L.L. Hench and J.M. Polak, *Biochem. Bioph. Res.* Co. 276, 461 (2000).

123. W.C.A. Vrouwenvelder, G.C. Groot and K. De Groot, *Biomaterials* 13, 382 (1992)

124. A. El Ghannam, P. Ducheyne and I.M. Shapiro, *Biomaterials* 18, 295 (1997).

125. E. Jallot, H. Benhayoune, L. Kilian, J.L. Irigaray, Y. Barbotteau, G. Balossier and P. Bonhomme, *J. Colloid Interf. Sci.* 233, 83 (2001).

126. O. Peitl, E.D. Zanotto and L.L. Hench, *J. Non-cryst. Solids* 292, 115 (2001).

127. E. Jallot, H. Benhayoune, L. Kilian, J.L. Irigaray, G. Balossier and P. Bonhomme, *J. Phys. D : Appl. Phys.* 33, 2775 (2000).

128. M. Ogino, F. Ohuchi and L.L. Hench, *J. Biomed. Mater. Res.* 14, 55 (1980).

129. O. Pietrement and E. Jallot, *Nanotechnology* 13, 18 (2002).

130. C. Ohtsuki, T. Kokubo and T. Yamamuro, *J. Non-cryst. Solids* 143, 84 (1992).

131. U. Gross and V. Strunz, *J. Biomed. Mater. Res. Symp.* 7, 503 (1985).

132. M. Vallet-Regi, I. Izquierdo-Barba and A.J. Salinas, *J. Biomed. Mater. Res.* 46, 560 (1999).

133. K. Kangasniemi and A. Yli-Urpo in Handbook of Bioactive Ceramics edited J. Wilson, CRC Press, Boston (1990), Vol. 1, p. 97.

134. D.C. Greenspan and L.L. Hench, *J. Biomed. Mater. Res.* 10, 503 (1976).

135. D. Avnir, L.C. Klein, D. Levy, U. Schubert and A.B. Wojcik in The chemistry of organosilicon compounds edited Y. Apeloig and Z. Rappoport, Wiley, Chichester, (1997), part. 2.

136. J. Livage, C. Roux, J.M. Da Costa, I. Desportes and J.E. Quinson, *J. Sol-Gel Sci. Technol.* 7, 45 (1996).

137. J.R. Jones and L.L. Hench, *Materials Science and technology* 17, 891 (2001).

138. M.M. Pereira and L.L. Hench, *J. Sol-gel Sci. Technol.* 7, 59 (1996).

139. M.M. Pereira, A.E. Clark and L.L. Hench, *J. Biomed. Mater. Res.* 28, 693 (1994).

140. L.L. Hench, D.L. Wheeler and D.C. Greenspan, *J. Sol-gel Sci. Technol.* 13, 245 (1998).

141. D.C. Greenspan, J.P. Zhong, Z.F. Chen and G.P. LaTorre in Proc. 10th Conf. on 'Bioceramics', L. Sedel and C. Rey eds., Oxford, Elsevier (1997).

142. L.L. Hench in Annuals of New York Academy of Science edited P. Ducheyne and J.E. Lemons 523 (1988).

143. T. Nakamura, T. Yamamuro, S. Higashi, T. Kokubo and S. Itoo, *J. Biomed. Mater. Res.* 19, 685 (1985).

144. T. Kokubo, S. Itoo, S. Sakka and T. Yamamuro, *J. Mater. Sci.* 21, 536 (1986).

145. T. Kitsugi, T. Yamamuro and T. Kokubo, *J. Bone Joint. Surg.* 71A, 264 (1989).

146. S. Yoshii, Y. Kakutani, T. Yamamuro, T. Nakamura, T. Kitsugi, M. Oka, T. Kokubo and M. Takagi, *J. Biomed. Mater. Res.* 22A, 327 (1988).

147. T. Kokubo, H. Kushitani, C. Ohtsuki, S. Sakka and T. Yamamuro, *J. Mater. Sci-Mater. Med.* 3, 79 (1992).

148. T. Kokubo, S. Ito, Z.T. Huang, T. Hayashi, S. Sakka, T. Kitsugi and T. Yamamuro, *J. Biomed. Mater. Res.* 24, 331 (1990).

149. P. Li, C. Ohtsuki, T. Kokubo, K. Nakanishi, N. Soga, T. Nakamura and T. Yamamuro, *J. Am. Ceram. Soc.* 75, 2094 (1992).

150. T. Kokubo, *J. Ceram. Soc. Jpn.* 99, 965 (1991).

151. M. Neo, S. Kotani, T. Nakamura and T. Yamamuro, *J. Biomed. Mater. Res.* 26, 1419 (1992).

152. M. Neo, S. Kotani, Y. Fujita, T. Nakamura and T. Yamamuro, *J. Biomed. Mater. Res.* 26, 255 (1992).

153. K.J.J. Pajamaki, T.S. Lindholm and O.H. Andersson, *J. Mater. Sci-Mater. Med.* 6, 14 (1995).

154. R.K. Iler in The Chemistry of Silica, John Wiley eds, New-York, 1979.

155. T. Kokubo, H. Kushitani, Y. Ebisawa, T. Kitsugi, S. Kotani, K. Oura and T. Yamamuro in Proc. 1st Int. Bioceramic Symposium, Ishiyaku Euroamerica, Tokyo, p. 157 (1989).

156. K. De Groot, R.G.T. Geesink, C.P.A.T. Klein and P. Serekian, *J. Biomed Mater. Res.* 21, 1375 (1987).

157. C.P.A.T. Klein, P. Patka, H.B.M. Van der Lubbe, J.G.C. Wolke and K. De Groot, *J. Biomed Mater. Res.* 25, 53 (1991).

158. K. Takatsuka, T. Yamamuro, T. Kitsugi, T. Nakamura, T. Shibuya and T. Goto, *J. Appl. Biomater.* 4, 317 (1993).

159. Y. Barbotteau, J.L. Irigaray and E . Jallot, *Surf. Interf. Anal.* 35, 450 (2003).

160. P. Ducheyne, W. Van Raemdonck, J.C. Heughbaert and M. Heughbaert, *Biomaterials* 7, 97 (1986).

161. K.A. Thomas, J.F. Kay, S.D. Cook and M. Jarcho, *J. Biomed. Mater. Res.* 21, 1395 (1987).

162. L. Jonasova, F.A. Müller, A. Helebrant, J. Strnad and P. Greil, *Biomaterials* 23, 3095 (2002).

163. P. Li, C. Ohtsuki, T. Kokubo, K. Nakanishi, N. Soga and K. De Groot, *J. Biomed. Mater. Res.* 28, 7 (1994).

164. P. Li, I. Kangasniemi, K. De Groot and T. Kokubo, *J. Am. Ceram. Soc.* 5, 1307 (1994).

165. T. Kokubo, F. Miyaji and H.M. Kim, *J. Am. Ceram. Soc.* 4, 1127 (1996).

166. H. Takadama, H.M. Kim, T. Kokubo and T. Nakamura, *J. Biomed. Mater. Res.* 57, 441 (2001).

167. E. Verne, C. Vitale Brovarone, C. Moisescu, E. Ghisolfi and E. Marmo, *Acta Mater.* 48, 4667 (2000).

168. L.L. Hench in the Bone-Biomaterials interface edited J.E. Davies, University of Toronto Press, Toronto (1991), p. 33.

169. B. Kasemo and J. Lausmaa in the Bone-Biomaterials interface edited J.E. Davies, University of Toronto Press, Toronto (1991), p. 19.

170. R.Z. Legeros, I. Orly, M. Gregoire and G. Daculsi in the Bone-Biomaterials interface edited J.E. Davies, University of Toronto Press, Toronto (1991), p. 76.

171. E. Jallot, *Applied Surface Science* 211, 89 (2003).

Tables captions

Table 1 : Ion concentrations (mmol/l) of biological solutions used to study physico-chemical reactions of bioactive materials.

Reprinted from Ref. 158. L. Jonasova et al., 'Hydroxyapatite formation on alkali-treated titanium with different content of Na^+ in the surface layer', Biomaterials 33, 3095 (2002), copyright (2002), with permission from Elsevier.

	Na^+	K^+	Mg^{2+}	Ca^{2+}	Cl^-	HCO_3^-	HPO_4^{2-}	SO_4^{2-}
Simulated body fluid, SBF	142	5	1	2.5	131	5	1	1
Human plasma	142	3.6-5.5	1	2.12-2.6	95-107	27	0.65-1.45	1

Table 1

Figures captions

Figure 1 : Comparison of interfacial thickness of reaction layer of bioactive implants bonded to bone or thickness of nonadherant fibrous tissue in contact with inactive bioceramics in bone.

Reprinted from Ref. 106. L.L. Hench, 'Bioceramics', J. Am. Ceram. Soc. 81, 1705, (1998), copyright 1998, with permission from The American Ceramic Society (www.ceramics.org.).

Figure 2 : STEM micrograph showing nanostructures of hydroxyapatite particles.

Figure 3 : Compositional dependence (in wt%) of bone bonding and soft tissue bonding of bioactive glasses and glass-ceramics. All compositions in region A are bioactive and bond to bone. They have constant 6wt% of P_2O_5. A/W glass-ceramic has higher P_2O_5 content. Compositions in region B are bioinert and lead to formation of a nonadherant fibrous capsule. Compositions in region C are resorbable. Region D is restricted by technical factors. Region E (soft tissue bonding) is inside the dashed line where the bioactivity is very high.

Reprinted from Ref. 106. L.L. Hench, 'Bioceramics', J. Am. Ceram. Soc. 81, 1705, (1998), copyright 1998, with permission from The American Ceramic Society (www.ceramics.org.).

Figure 4 : Sequence of interfacial reactions involved in forming a bond between tissue and bioactive ceramics.

Reprinted from Ref. 12. L.L. Hench, 'Biomaterials: a forecast for the future', Biomaterials 19, 1419 (1998), copyright (1998), with permission from Elsevier.

Figure 5 : Schematic illustration of the surface stages (I-V) reactions on bioactive glass, forming double SiO_2-rich and Ca,P-rich layers.

Reprinted from Ref. 126. O. Peitl et al., 'Highly bioactive P_2O_5-Na_2O-CaO-SiO_2 glass-ceramics', Journal of Non-Cryst. Solids 292, 115 (2001), copyright (2001), with permission from Elsevier.

Figure 6 : STEM micrograph of bioactive glass particles immersed in a biological solution during four days. The particles are in dissolution and an electron dense layer appears (apatite layer).

Figure 7 : Schematic representation of surface structure of A-W exposed to body fluid.

Reprinted from Ref. 29. T. Kokubo, 'Surface chemistry of bioactive glass-ceramics', Journal of Non-Cryst. Solids 120, 138 (1990), copyright (1990), with permission from Elsevier.

Figure 8 : Schematic representation of formation of apatite layer on the surface of A-W.

Reprinted from Ref. 29. T. Kokubo, 'Surface chemistry of bioactive glass-ceramics', Journal of Non-Cryst. Solids 120, 138 (1990), copyright (1990), with permission from Elsevier.

Figure 9 : Possible structural changes of the titanium surface (a), during acid etching (b), alkali treatment (c), and subsequent apatite formation in SBF (d-f).

Reprinted from Ref. 158. L. Jonasova et al., 'Hydroxyapatite formation on alkali-treated titanium with different content of Na^+ in the surface layer', Biomaterials 33, 3095 (2002), copyright (2002), with permission from Elsevier.

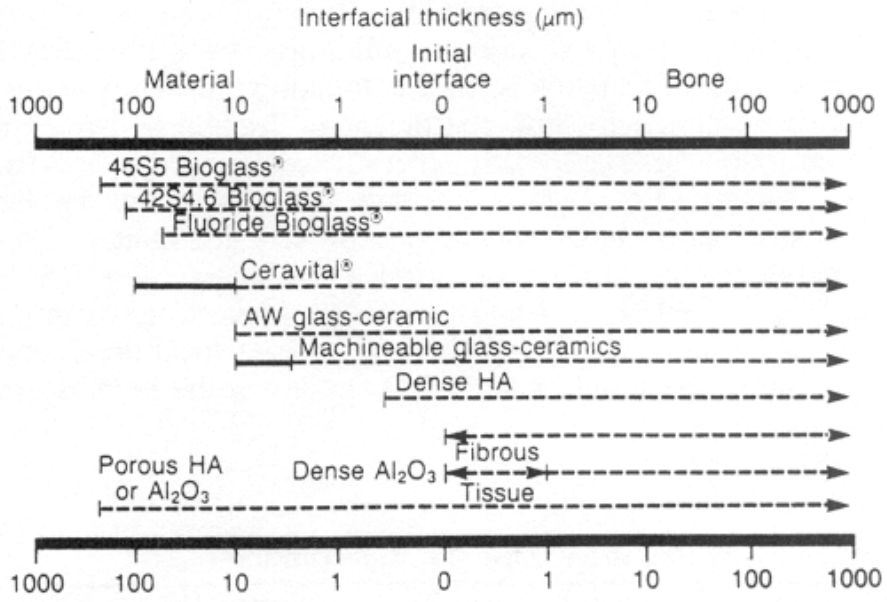
Interfacial thickness (μm)
Material
Initial interface
Bone
1000
100
10
1
0
1
10
100
1000
45S5 Bioglass®
42S4.6 Bioglass®
Fluoride Bioglass®
Ceravital®
AW glass-ceramic
Machineable glass-ceramics
Dense HA
Fibrous Tissue
Porous HA or Al_2O_3
Dense Al_2O_3

Figure 1

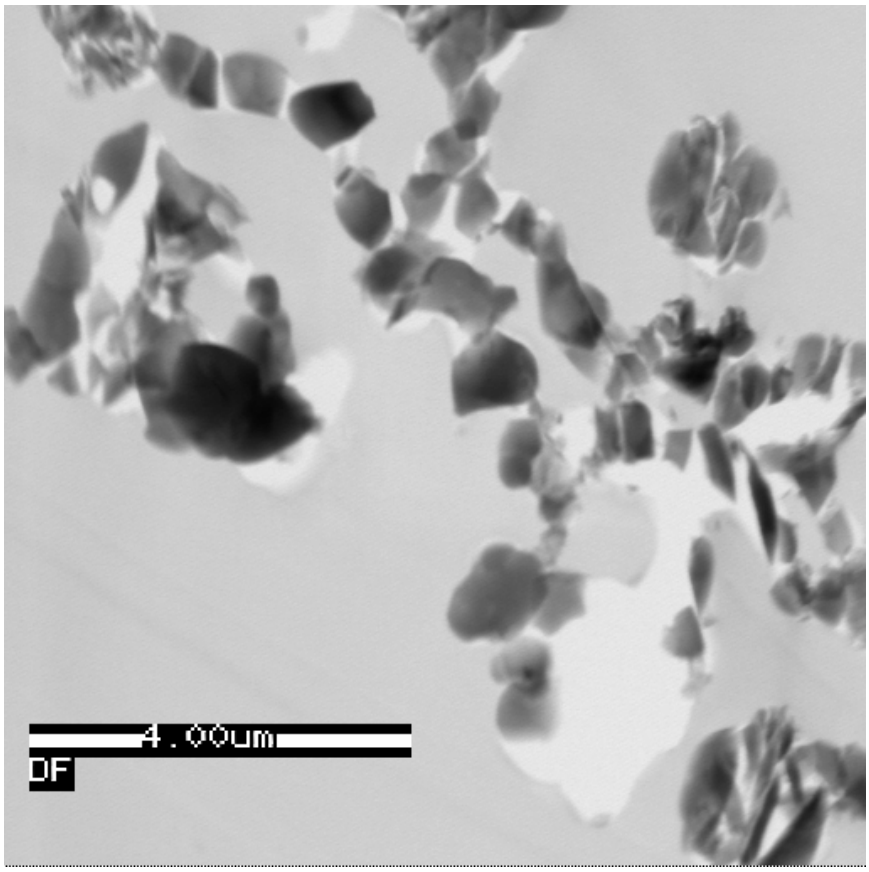

Figure 2

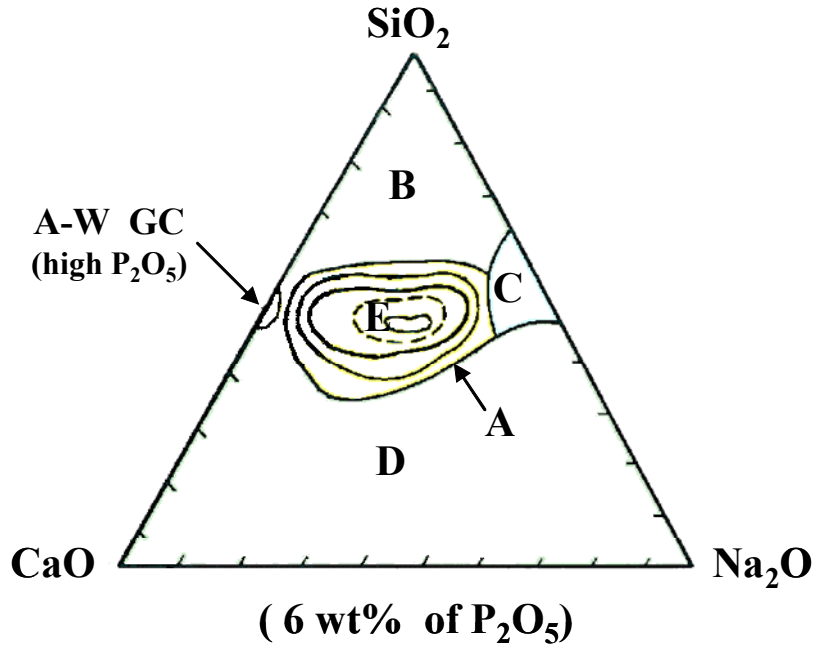

Figure 3

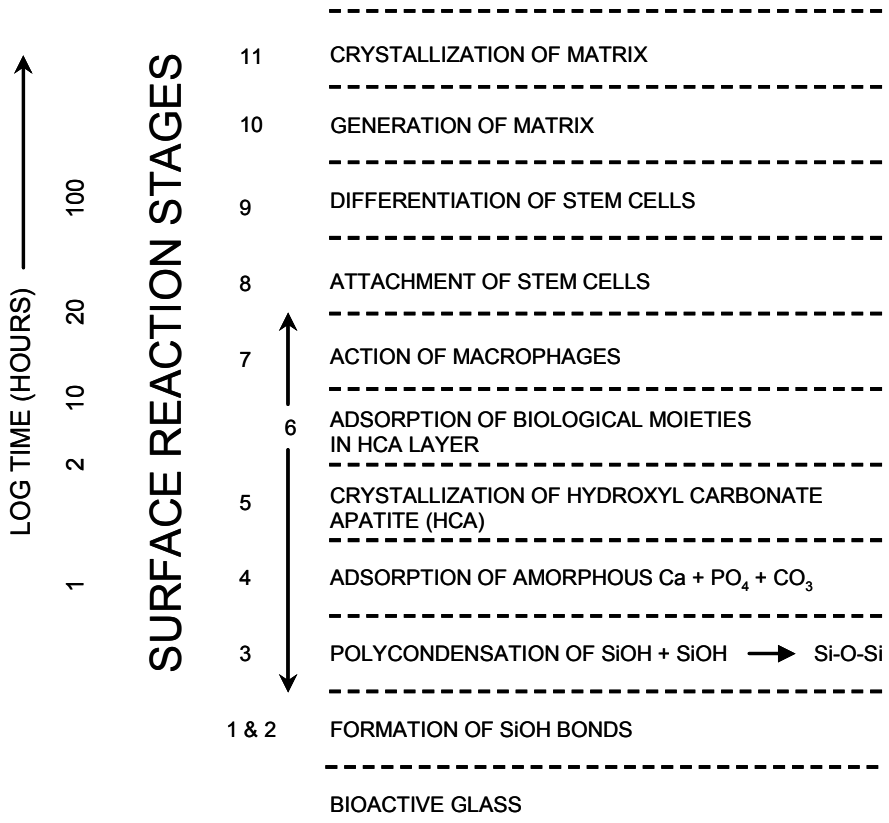
LOG TIME (HOURS)
1
2
10
20
100
SURFACE REACTION STAGES
11
CRYSTALLIZATION OF MATRIX
10
GENERATION OF MATRIX
9
DIFFERENTIATION OF STEM CELLS
8
ATTACHMENT OF STEM CELLS
7
ACTION OF MACROPHAGES
6
ADSORPTION OF BIOLOGICAL MOIETIES IN HCA LAYER
5
CRYSTALLIZATION OF HYDROXYL CARBONATE APATITE (HCA)
4
ADSORPTION OF AMORPHOUS Ca + PO4 + CO3
3
POLYCONDENSATION OF SiOH + SiOH → Si-O-Si
1 & 2
FORMATION OF SiOH BONDS
BIOACTIVE GLASS

Figure 4

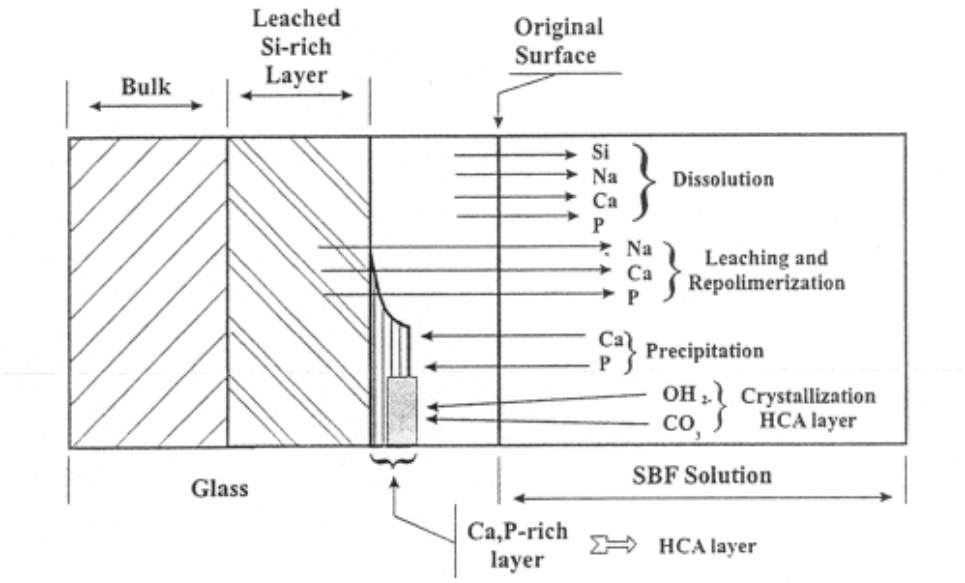
Leached
Si-rich
Layer
Original
Surface
Bulk
Si
Na
Ca
P
Dissolution
Na
Ca
P
Leaching and
Repolimerization
Ca
P
Precipitation
OH
CO3
Crystallization
HCA layer
Glass
SBF Solution
Ca,P-rich
layer
HCA layer

Figure 5

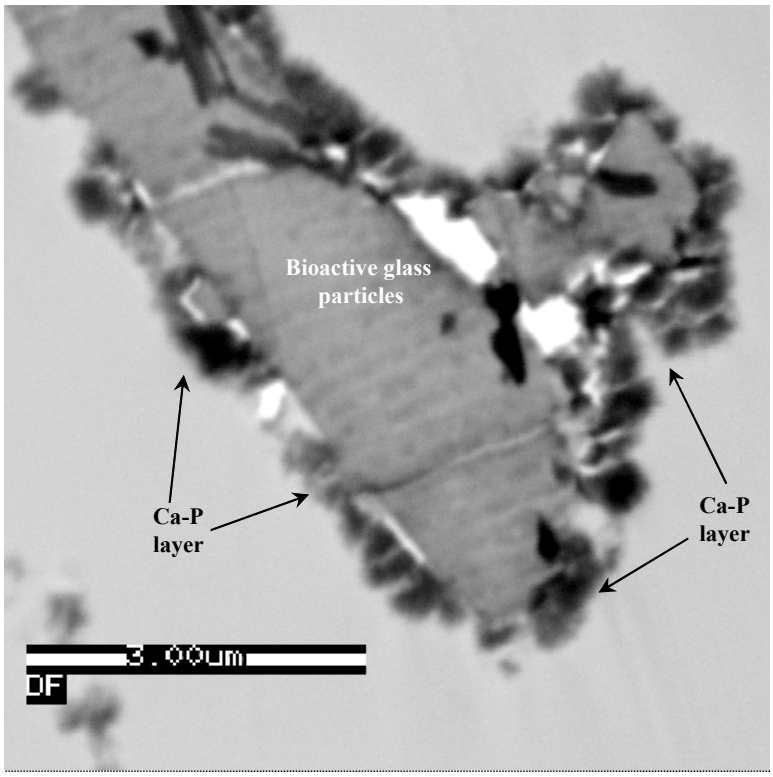

Figure 6

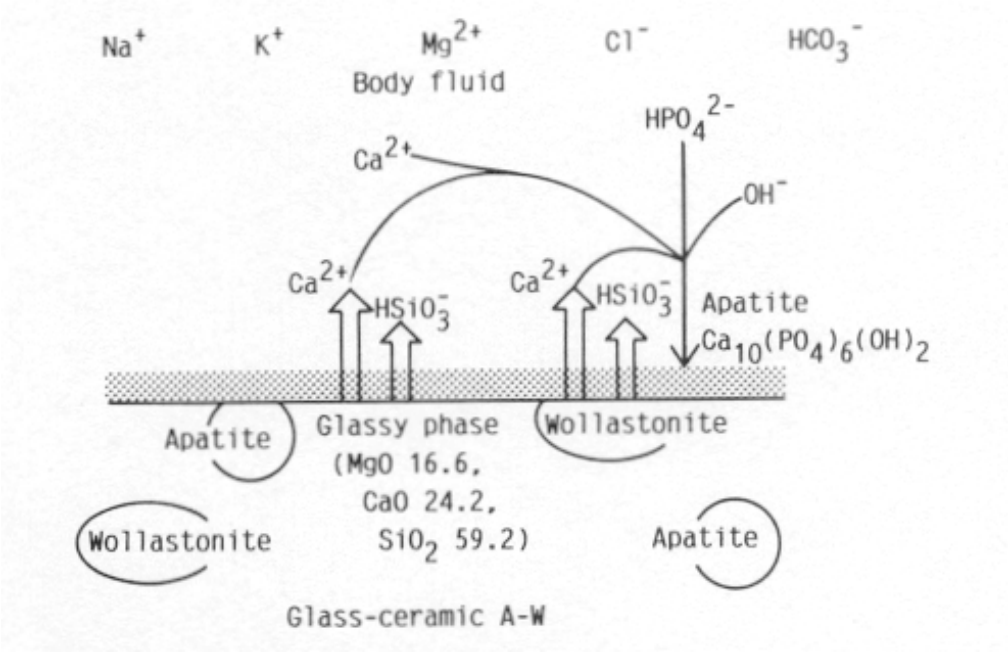
Na+
K+
Mg2+
Cl-
HCO3-
Body fluid
HPO4 2-
Ca2+
OH-
Ca2+
HSiO3-
Ca2+
HSiO3-
Apatite
Ca10(PO4)6(OH)2
Apatite
Glassy phase
(MgO 16.6,
CaO 24.2,
SiO2 59.2)
Wollastonite
Wollastonite
Apatite
Glass-ceramic A-W

Figure 7

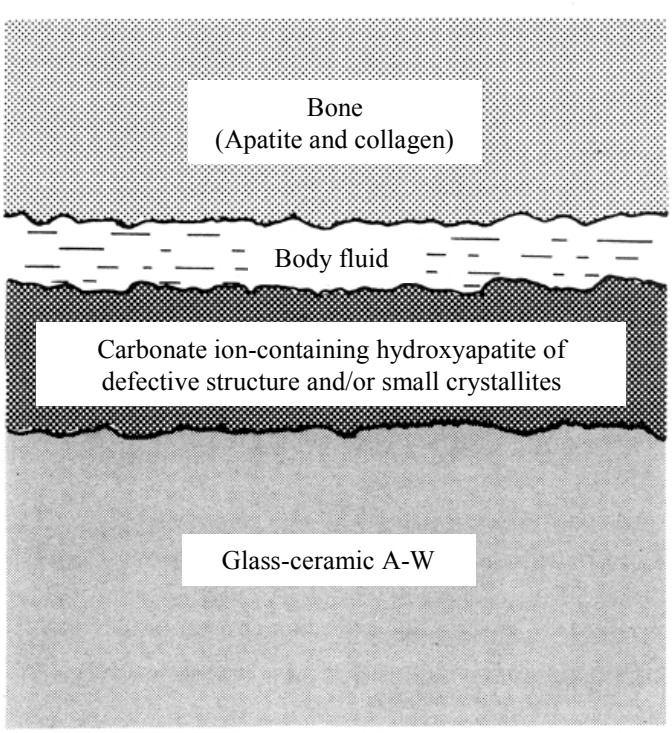
Bone
(Apatite and collagen)
Body fluid
Carbonate ion-containing hydroxyapatite of
defective structure and/or small crystallites
Glass-ceramic A-W

Figure 8

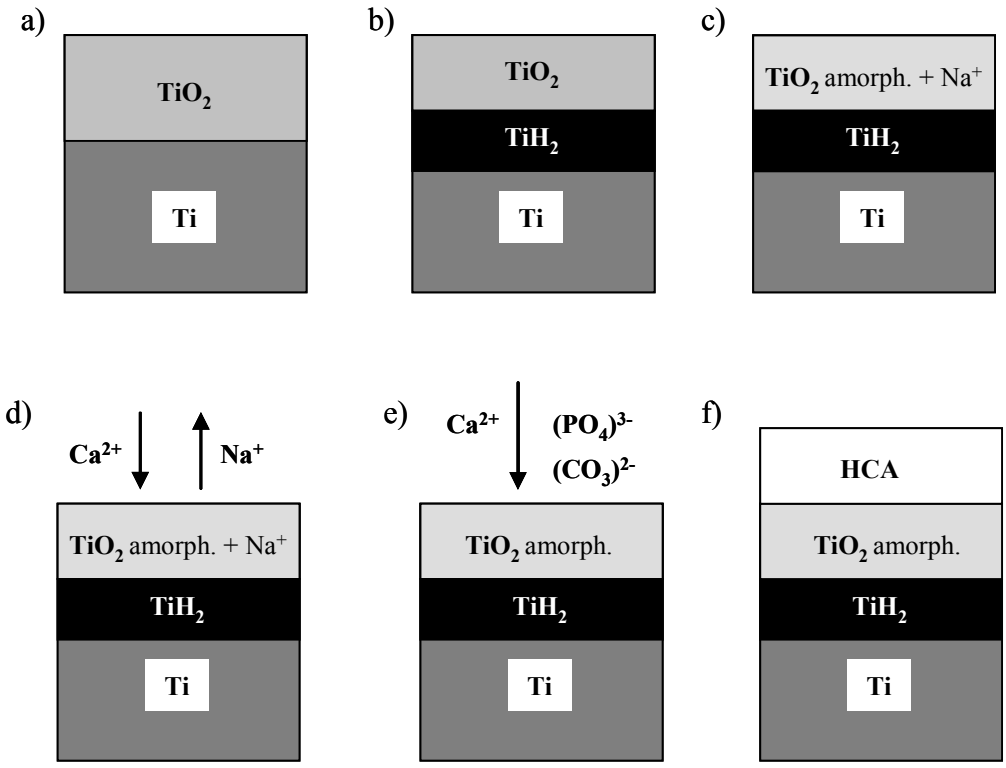
a)
TiO2
Ti
b)
TiO2
TiH2
Ti
c)
TiO2 amorph. + Na+
TiH2
Ti
d)
Ca2+
Na+
TiO2 amorph. + Na+
TiH2
Ti
e)
Ca2+
(PO4)3-
(CO3)2-
TiO2 amorph.
TiH2
Ti
f)
HCA
TiO2 amorph.
TiH2
Ti

Figure 9